

This item was submitted to Loughborough's Institutional Repository (<https://dspace.lboro.ac.uk/>) by the author and is made available under the following Creative Commons Licence conditions.



**CC creative commons**  
COMMONS DEED

**Attribution-NonCommercial-NoDerivs 2.5**

**You are free:**

- to copy, distribute, display, and perform the work

**Under the following conditions:**

**BY:** **Attribution.** You must attribute the work in the manner specified by the author or licensor.

**Noncommercial.** You may not use this work for commercial purposes.

**No Derivative Works.** You may not alter, transform, or build upon this work.

- For any reuse or distribution, you must make clear to others the license terms of this work.
- Any of these conditions can be waived if you get permission from the copyright holder.

**Your fair use and other rights are in no way affected by the above.**

This is a human-readable summary of the [Legal Code \(the full license\)](#).

[Disclaimer](#) 

For the full text of this licence, please go to:  
<http://creativecommons.org/licenses/by-nc-nd/2.5/>

## Reducing extrinsic hysteresis in first-order $\text{La}(\text{Fe}, \text{Co}, \text{Si})_{13}$ magnetocaloric systems

J. D. Moore,<sup>1,a)</sup> K. Morrison,<sup>1</sup> K. G. Sandeman,<sup>1</sup> M. Katter,<sup>2</sup> and L. F. Cohen<sup>1</sup>

<sup>1</sup>The Blackett Laboratory, Imperial College, London SW7 2AZ, United Kingdom

<sup>2</sup>Vacuumschmelze GmbH & Co. KG, Grüner Weg 37, 63450 Hanau, Germany

(Received 15 October 2009; accepted 1 December 2009; published online 23 December 2009)

Simultaneous magnetization and sample temperature measurements were performed as a function of magnetic field and magnetic field sweep-rates to study the influence of these conditions on the hysteresis of the magnetocaloric transition in  $\text{La}(\text{Fe}_{1-x-y}\text{Co}_x\text{Si}_y)_{13}$  samples. The large magnetocaloric effect in the compounds that show a first-order transition cause a significant departure from isothermal conditions leading to dynamic sweep-rate dependent magnetic hysteresis. Here we show how this deleterious effect can be greatly reduced by changing the sample geometry or by use of materials which show a second-order transition only. The key signatures of nonisothermal conditions in the magnetization data are highlighted. © 2009 American Institute of Physics. [doi:10.1063/1.3276565]

The magnetocaloric effect (MCE) is the change in temperature ( $\Delta T$ ) of a magnetic material caused by applying a magnetic field ( $H$ ). The effect is greatest at temperatures near a magnetic phase transition and is known as the giant magnetocaloric effect when a first-order magneto-structural transformation takes place. The discovery of giant MCE in  $\text{Gd}_5(\text{Si}_2\text{Ge}_2)$  in 1997 by Pecharsky *et al.*<sup>1</sup> stimulated intense research in this area because of the potential of these materials for application in near-room temperature magnetic refrigeration (MR).

The ideal combination of properties for a magnetocaloric material for cooling applications are, a large magnetization change  $\Delta M$  in a small externally applied field, a low intrinsic magnetic hysteresis  $\Delta H_{\text{int}}$ , high thermal conductivity and low heat capacity. The first two conditions are satisfied in the very interesting class of materials  $\text{La}(\text{Fe}, \text{Si})_{13}$ .<sup>2-4</sup> What is not widely appreciated is that in a MR cycle the magnetizing and demagnetizing steps are dynamic and the rate of field change is high  $\dot{H} > 1$  T/s. Therefore understanding the dynamics of the system and the impact on performance when the system is driven out of equilibrium with the thermal bath, are extremely important for application. Here, we demonstrate using the magnetocaloric  $\text{La}(\text{Fe}_{1-x-y}\text{Co}_x\text{Si}_y)_{13}$  materials<sup>5</sup> that the dynamics of heat exchange with the material undergoing a field-driven transition leads to a significant sweep-rate dependent extrinsic magnetic hysteresis. The observations stem from the time needed to extract heat from the sample, which directly relates to the heat capacity and thermal conductivity.<sup>6</sup> This extrinsic contribution is a vital consideration for some material systems, and is often overlooked when comparing different candidate MCE materials under different experimental conditions. Here we demonstrate the use of a probe that simultaneously measures sample temperature change  $\Delta T$  and magnetization and show that the thermal management of the system can be significantly improved by changing sample geometry or moving to compositions that show only a second order phase transition.

There is limited discussion in the literature on the sweep rate dependence of MCE (i.e.,  $\Delta T$ ).<sup>7-9</sup> Dynamics of first-order transition have been studied by pulsed-magnetic-field in the arrested state at low temperature in  $\text{Gd}_5\text{Ge}_4$ ,<sup>10,11</sup> and by magnetic relaxation measurements, for example in  $\text{LaFe}_{11.7}\text{Si}_{1.3}$  (Ref. 12) and  $\text{Gd}_5\text{Si}_2\text{Ge}_2$ .<sup>13</sup> For the latter case the dynamic behavior was considered to be due to thermal activation over the energy barrier between different magnetic phases. Thermodynamic models of MR cycles also do not usually consider sweep rate dependence or the finite rate of heat transfer.<sup>14,15</sup>

Here we study two large, pressed and sintered plates of  $\text{La}(\text{Fe}, \text{Co}, \text{Si})_{13}$  prepared by powder metallurgy as described elsewhere.<sup>5</sup>  $\text{LaFe}_{11.71}\text{Co}_{0.19}\text{Si}_{1.11}$  referred to as LaFeCoSi-1 (size  $3 \times 3 \times 1$  mm<sup>3</sup>) undergoes first-order phase transition with a Curie temperature  $T_c \sim 202$  K.  $\text{LaFe}_{10.97}\text{Co}_{1.03}\text{Si}$  (size  $2.1 \times 1.8 \times 1$  mm<sup>3</sup>) has second-order phase transition at  $T_c \sim 293$  K and is referred to as LaFeCoSi-2. After measurements on LaFeCoSi-1 and LaFeCoSi-2 were completed the plates were broken into small pieces and a fragment from each with diameter 200  $\mu\text{m}$  was chosen for study. Finally for comparison we have studied a needle-shaped piece of 7.8 mg polycrystalline gadolinium (Gd) with  $T_c \sim 294$  K. Simultaneous  $M(H)$  and sample temperature measurements were performed using a VSM (field resolution  $\pm 0.1$  mT at 0.7 T/min sweep-rate) in combination with a Pt100 platinum resistance thermometer (sensitivity  $\pm 0.01$  K) mounted on an Alumina block (size  $1.6 \times 1.2 \times 1.1$  mm<sup>3</sup>) attached to the free surface of the plate using thin layer of GE varnish. The Pt100 sensor underestimates the sample temperature as it is comparable in size and in thermal mass to the plate. The other surface of the sample was attached to the polymer holder. All samples were oriented in field to minimize demagnetizing effects.

At 209 K LaFeCoSi-1 shows a first-order paramagnetic (PM) to ferromagnetic (FM) transition at  $H \sim 2$  T bound by the transition fields  $H_{C1}$  and  $H_{C2}$  on the upwards field-leg and  $H_{C3}$  and  $H_{C4}$  on the downwards field-leg, as indicated in Fig. 1(a). The key feature of these  $M(H)$  loops is the fanning out of the curve in the transition region as  $\dot{H}$  is increased.

<sup>a)</sup>Electronic mail: james.moore@imperial.ac.uk.

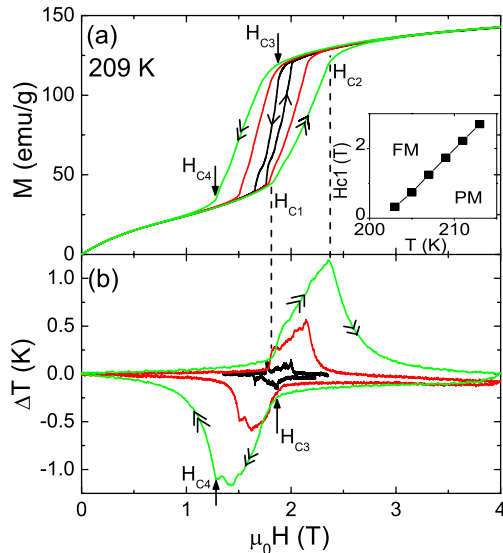


FIG. 1. (Color online) (a)  $M(H)$  loops for sample LaFeCoSi-1 taken at 209 K; the narrow inner loop is at 0.02 T/min (indicated by single arrows); the middle loop is at 0.2 T/min; and the wide outer loop is at 0.7 T/min (indicated by double arrows). The critical fields  $H_{C1}$  to  $H_{C4}$  are indicated for the 0.7 T/min curve. Inset to (a) shows temperature dependence of  $H_{C1}(T)$ . (b) Sample temperature  $\Delta T$  relative to the bath  $T$ . The three loops correspond to the  $M(H)$  loops in part (a).

This feature is directly connected with the change in sample temperature  $\Delta T$  due to the MCE shown in Fig. 1(b). As  $\dot{H}$  is increased the sample reaches a higher temperature due to the finite rate of heat exchange with the bath, so that although  $H_{C1}$  remains constant, (because MCE in the PM phase is small)  $H_{C2}$  shifts to higher field, and the phase line  $H_{C2}(T)$  becomes sweep-rate dependent. The inset to Fig. 1(a) shows the steep  $dH_c/dT$  in this system, and this factor along with the large MCE contributes to the high  $\dot{H}$  dependence we observe. At fields above  $H_{C2}$  the transition is complete and the  $\Delta T$  returns gradually toward the bath  $T$ . The  $M(H)$  curve on the downwards field-leg behaves in a similar fashion with a rate-dependent  $H_{C4}$  as the sample cools.

It is well known that temperature hysteresis is expected in a first-order phase transition where there is latent heat as it is a thermodynamic requirement that the transitions on warming and on cooling be separated on a thermodynamic temperature scale, as discussed by Pecharsky *et al.*<sup>16</sup> The fanning-out feature that we see in  $M(H)$  is a reflection of this basic thermodynamic requirement.

In Fig. 2(a) we show the average magnetic hysteresis  $\Delta H$  extracted from  $M(H)$  curves for the LaFeCoSi-1 plate and the 200  $\mu\text{m}$  fragment both versus  $\dot{H}$  at 209 K. For  $\dot{H} < 0.1$  T/min the measurement conditions are approximately isothermal and  $\Delta H \sim \Delta H_{\text{int}}$ , which is low in these materials compared to other giant magnetocaloric systems. At higher  $\dot{H}$  the magnetic hysteresis is given by,

$$\Delta H = \Delta H_{\text{int}} + \Delta H_{\text{ext}} = \Delta H_{\text{int}} + (dH_c/dT) \times \Delta T, \quad (1)$$

where  $\Delta H_{\text{ext}}$  is the extrinsic magnetic hysteresis. Note that Eq. (1) does not include hysteresis associated with strain or kinetic nucleation barriers.<sup>9,17</sup> It is also assumed the sample temperature returns to the bath temperature before the reverse field-leg commences. Equation (1) was fitted to the  $\Delta T$  values extracted from Fig. 1(b) and as shown in Fig. 2(a) it

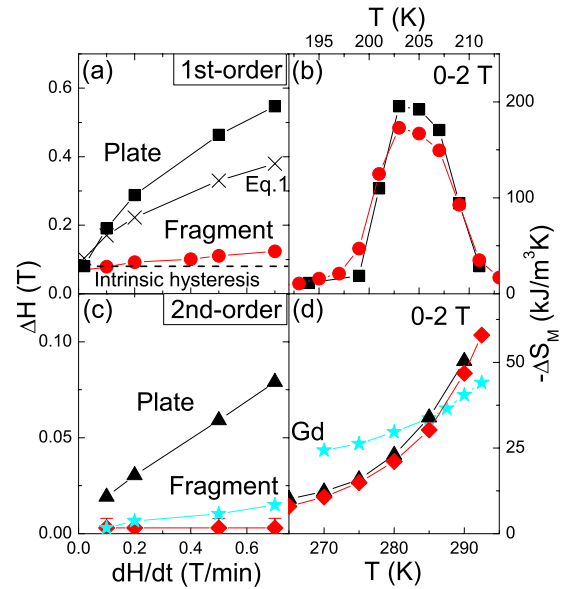


FIG. 2. (Color online) Magnetic field hysteresis  $\Delta H$  vs the field sweep-rate for (a) LaFeCoSi-1 plate (square) and fragment (circle) at 209 K, and (c) LaFeCoSi-2 plate (triangle) and fragment (diamond) and Gd needle (star) samples at 295 K. The LaFeCoSi-1 data is fitted by Eq. (1) (crosses) in part (a). The magnetic entropy change  $\Delta S_M$  in 2 T field change vs temperature  $T$  for (b) LaFeCoSi-1 plate and fragment, and (d) LaFeCoSi-2 plate and fragment and Gd needle samples.

agrees qualitatively with the curve for the LaFeCoSi-1 plate. However the fit to Eq. (1) underestimates  $\Delta H_{\text{ext}}$  by  $\sim 35\%$  because the Pt100 sensor underestimates the real sample  $\Delta T$ . In particular, maximum  $\Delta H$  will be observed when  $\Delta T = \Delta T_{\text{ad}}$  in Eq. (1) which gives  $\Delta H \sim 1.1$  T for  $\Delta T_{\text{ad}} = 4$  K.<sup>18</sup> Unfortunately, the essential factors that contribute to  $\Delta H_{\text{ext}}$  are those that are attractive for MR application, namely steep  $dH_c/dT$  and large  $\Delta T$ . However, in systems where  $\Delta H = \Delta H_{\text{int}} + \Delta H_{\text{ext}}$  is dominated by a large  $\Delta H_{\text{int}}$  contribution, the effect we are describing here is less significant and probably it is this factor that explains why it has gone unreported. In this important material system this combination of parameters means that the  $\Delta H_{\text{ext}}$  term can be extremely important. However, a simple geometric change to the samples by fragmentation removes a significant component of extrinsic hysteresis. Most importantly Fig. 2(b) shows that fragmentation does not impair the entropy change  $\Delta S_M$  (taken from magnetization data) associated with the magnetocaloric transition and hence fragments or equivalent low thermal mass geometries would seem more attractive for application.  $\Delta H_{\text{ext}}$  should also be reduced by using fluid, for example water (typical prototype coolant), rather than nitrogen gas (typical research laboratory cryogenic environment).

Figure 2(c) shows the average  $\Delta H$  versus  $\dot{H}$  for the second-order materials LaFeCoSi-2 and the Gd needle taken at 295 K. Noticeably the  $\Delta H_{\text{ext}}$  is much smaller in bulk LaFeCoSi-2 compared to LaFeCoSi-1 because the  $\Delta T$  peak is both typically smaller for second-order transitions and is spread out over a wider field and temperature range.  $\Delta H_{\text{ext}}$  is further reduced for the LaFeCoSi-2 fragment and for the Gd needle demonstrating that even for second order materials, sample geometry, and thermal mass are paramount. The  $\Delta S_M$  shown in Fig. 2(d) are consistent with values reported elsewhere.<sup>5,19</sup>

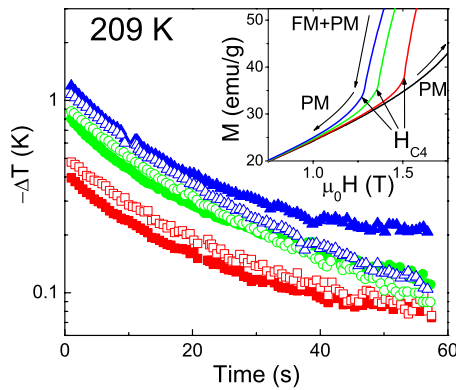


FIG. 3. (Color online) Open symbols show change in sample temperature  $\Delta T$  measured by the Pt100 sensor as the field is reduced from  $H_{C4}$  to zero ( $t=0$  corresponds to  $H=H_{C4}$ ) for LaFeCoSi-1 at 209 K (squares  $-0.2$  T/min, circles  $-0.5$  T/min, and triangles  $-0.7$  T/min). Closed symbols show  $\Delta T$  extracted from change in paramagnetic moment in  $M(H)$  over the same field range. Inset illustrates the effect of field sweep-rate on the paramagnetic moment in  $M(H)$ .

Signature of sample heating is also evident from the apparent hysteresis in the PM region of the  $M(H)$  curve (true also for the FM region) for LaFeCoSi-1. The inset to Fig. 3 highlights the difference for field sweep direction and comparison with Fig. 1(b) reveals that the change in moment  $\Delta M$  is due to the sample  $T$  slowly returning toward the bath  $T$ . In order to extract  $\Delta T$  from the  $M(H)$  loops in the PM phase, we first take a series of isothermal  $M(H)$  curves so that the change in PM moment with temperature  $PM(T)$  is known. We then extracted  $\Delta M$  from the increasing and decreasing field legs below  $H_{C4}$  and infer the sample temperature and therefore  $\Delta T$ , using the known  $PM(T)$  curve. The main part of Fig. 3 plots  $\Delta T$  extracted from  $M(H)$  and  $\Delta T$  measured by the Pt100 sensor, both versus the real time during the experiment where  $t=0$  was started at  $H_{C4}$  and increasing  $t$  corresponds to decreasing  $H$ . There is excellent agreement between the two independent measures of  $\Delta T$ . From the data in the first 20 s in Fig. 3 we estimate the time constant for  $\Delta T$  to decrease to  $1/e$  of its initial value as  $\tau \sim 15$  s, which although system specific is surprisingly long highlighting that heat exchange is an important consideration when comparing MCE materials measured in the laboratory environment.

Although dynamic behavior of magnetization in first-order magnetic phase transition has been previously interpreted in terms of thermal activation over an energy barrier between magnetic phases,<sup>12,13</sup> our work shows that sample heating is the dominant cause of dynamic effects in La(Fe,Co,Si)<sub>13</sub> samples with large thermal mass due to the combination of small  $\Delta H_{\text{int}}$  and large  $dH_c/dT$  and MCE. On a similar note, melt-spinning has been shown to significantly reduce hysteresis in La(Fe,Si)<sub>13</sub>-based alloys compared to bulk material,<sup>20</sup> and it is likely that this is at least in part because thin ribbons behave similarly to the LaFeCoSi-1 fragment where  $\Delta H_{\text{ext}}$  is suppressed due to the large surface area and small thermal mass.

Previously we have shown fragmentation in the prototype magnetocaloric Gd<sub>5</sub>Ge<sub>4</sub> reduces internal strain and low-

ers the operating field.<sup>21</sup> Here we demonstrate that heat exchange is critical to the dynamics in MCE materials and that this leads to a rate-dependent  $\Delta H_{\text{ext}}$ . This hysteresis is largest in materials where  $dH_c/dT$  and  $\Delta T_{\text{ad}}$  are high, which are also the properties attractive for MR application. The contribution of  $\Delta H_{\text{ext}}$  should be reduced by improving sample geometry, such as through increasing surface area to volume ratio, or by having  $\Delta T(H)$  spread out over a wider field range. The key feature of nonisothermal conditions for first-order transitions is the fanning-out in  $M(H)$  with rate-dependent  $H_{C2}$  and  $H_{C4}$ , and care should be taken to minimize this artifact in supposedly isothermal magnetization measurements.

This work was supported by the European Commission Grant No. FP7 CP-FP 214864-2 Solid State Energy Efficient Cooling (SSEEC). The authors thank Neil Wilson from Cambridge for supplying Gd sample and for stimulating discussion.

- <sup>1</sup>V. K. Pecharsky and K. A. Gschneidner, Jr., *Phys. Rev. Lett.* **78**, 4494 (1997).
- <sup>2</sup>F. X. Hu, B. G. Shen, J. R. Sun, Z. H. Cheng, G. H. Rao, and X. X. Zhang, *Appl. Phys. Lett.* **78**, 233675 (2001).
- <sup>3</sup>S. Fujieda, A. Fujita, and K. Fukamichi, *Appl. Phys. Lett.* **81**, 1276 (2002).
- <sup>4</sup>O. Gutfleisch, A. Yan, and K. H. Müller, *J. Appl. Phys.* **97**, 10M305 (2005).
- <sup>5</sup>M. Katter, V. Zellmann, G. W. Reppel, and K. Uestuener, *IEEE Trans. Magn.* **44**, 3044 (2008).
- <sup>6</sup>S. Fujieda, Y. Hasegawa, and A. Fujita, and K. Fukamichi, *J. Appl. Phys.* **95**, 2429 (2004).
- <sup>7</sup>A. M. Tishin, A. V. Derkach, Y. I. Spichkin, M. D. Kuz'min, A. S. Chernyshov, K. A. Gschneidner, Jr. and V. K. Pecharsky, *J. Magn. Mater.* **310**, 2800 (2007).
- <sup>8</sup>Y. I. Spichkin, I. Zubkov, A. M. Tishin, K. A. Gschneidner, Jr., and V. K. Pecharsky, in *Proceedings of the Third International Conference on Magnetic Refrigeration at Room Temperature*, edited by P. Egolf (International Institute of Refrigeration, Paris, 2009).
- <sup>9</sup>S. Madireddi, M. Zhang, V. K. Pecharsky, and K. A. Gschneidner, Jr., in *Proceedings of the Third International Conference on Magnetic Refrigeration at Room Temperature*, edited by P. Egolf (International Institute of Refrigeration, Paris, 2009).
- <sup>10</sup>Z. W. Ouyang, H. Nojiri, S. Yoshii, G. H. Rao, Y. C. Wang, V. K. Pecharsky, and K. A. Gschneidner, Jr., *Phys. Rev. B* **77**, 184426 (2008).
- <sup>11</sup>Z. W. Ouyang, V. K. Pecharsky, K. A. Gschneidner, D. L. Schlagel, and T. A. Lograsso, *Phys. Rev. B* **76**, 134406 (2007).
- <sup>12</sup>H. W. Zhang, F. Wang, T. Y. Zhao, S. Y. Zhang, J. R. Sun, and B. G. Shen, *Phys. Rev. B* **70**, 212402 (2004).
- <sup>13</sup>J. Leib, J. E. Snyder, T. A. Lograsso, D. Schlagel, and D. C. Jiles, *J. Appl. Phys.* **95**, 6915 (2004).
- <sup>14</sup>V. Basso, C. P. Sasso, G. Bertotti, and M. Lobue, *Int. J. Refrig.* **29**, 1358 (2006).
- <sup>15</sup>A. M. Rowe and J. A. Barclay, *J. Appl. Phys.* **93**, 1672 (2003).
- <sup>16</sup>V. K. Pecharsky, K. A. Gschneidner, Jr., and D. Fort, *Scr. Mater.* **35**, 843 (1996).
- <sup>17</sup>K. A. Gschneidner, Jr., V. K. Pecharsky, E. Bruck, H. G. M. Duijn, and E. M. Levin, *Phys. Rev. Lett.* **85**, 4190 (2000).
- <sup>18</sup>F. X. Hu, M. Ilyn, A. M. Tishin, J. R. Sun, G. J. Wang, Y. F. Chen, F. Wang, Z. H. Cheng, and B. G. Shen, *J. Appl. Phys.* **93**, 095503 (2003).
- <sup>19</sup>K. A. Gschneidner, Jr. and V. K. Pecharsky, *Annu. Rev. Mater. Sci.* **30**, 387 (2000).
- <sup>20</sup>J. Lyubina, O. Gutfleisch, M. D. Kuz'min, and M. Richter, *J. Magn. Mater.* **320**, 2252 (2008).
- <sup>21</sup>J. D. Moore, G. K. Perkins, Y. Bugoslavsky, M. K. Chattopadhyay, S. B. Roy, P. Chaddah, V. K. Pecharsky, K. A. Gschneidner, Jr., and L. F. Cohen, *Appl. Phys. Lett.* **88**, 072501 (2006).